

GT2004-54295

COMPRESSOR STALL CONTROL THROUGH ENDWALL RECIRCULATION

Anthony J. Strazisar
NASA-Glenn Research Center
Cleveland, Ohio, USA

Michelle M. Bright
NASA-Glenn Research Center
Cleveland, Ohio, USA

Scott Thorp
NASA-Glenn Research Center
Cleveland, Ohio, USA

Dennis E. Culley
NASA-Glenn Research Center
Cleveland, Ohio, USA

Kenneth L. Suder
NASA-Glenn Research Center
Cleveland, Ohio, USA

ABSTRACT

Experiments that demonstrate the use of endwall recirculation to control the stall of transonic compressor stages are described. Endwall recirculation of a compressor stage is implemented by bleeding air from the casing downstream of a stator blade row and injecting the air as a wall jet upstream of a preceding rotor blade row. The bleed ports, injection ports, and recirculation channels are circumferentially discrete, and occupy only 20-30% of the circumference. The development of compact wall-jet injectors is described first. Next, the results of proof-of-concept steady recirculation tests on a single-stage transonic compressor are presented. Finally, the potential for using endwall recirculation to increase the stability of transonic highly-loaded multistage compressors is demonstrated through results from a rig test of simulated recirculation driving both a steady injected flow and an unsteady injected flow commanded by closed-loop active control during compressor operation at 78-100% of design speed. In this test air from an external source was injected upstream of several rotor blade rows while compressor bleed was increased by an amount equivalent to the injected massflow. During closed loop control, wall static pressure fluctuations were monitored and the injected flow rate was controlled to reduce the stalling mass flow. The use of wall jet injection to study the dynamics of transonic compressor stages is also discussed.

INTRODUCTION

Adequate stability is an important feature of any compressor design. The desire to reduce compressor size, weight, and complexity by reducing the number of stages and eliminating variable vanes leads to higher loading per stage and more severe matching problems. For these reasons, there has been a fairly constant activity over the last decade devoted to the early detection of compressor instability and to the development of active and passive techniques aimed at increasing stability.

Many of these techniques feature injection of air into the tip region of compressor rotors, since high pressure air is readily available from compressor bleeds.

Weigl [1] and Spakovszky [2,3] demonstrated successful control of stall in a single stage transonic compressor using feedback control of wall jet injectors located upstream of the rotor. They used inputs derived from high-response pressure transducers located upstream of the rotor to control long wavelength, modal disturbances for clean, radially distorted, and circumferentially distorted inlet flows through a combination of steady injection and controlled unsteady injection. Suder [4] used the same test hardware to study the impact of jet injection velocity and injector arrangement around the circumference. The injection air for all of these efforts was supplied by an ambient temperature air source external to the compressor. Suder found that maintaining choked flow in the injectors yielded the greatest stability increase and also found that the number of injectors and the total injected flow could be reduced relative to that used in [1-3] with no loss in stability enhancement. These results are significant because in an engine implementation injected air would be supplied by compressor bleed and the efficiency penalty associated with increased bleed makes any reduction in the amount of injected air required to achieve stall control desirable.

As a first step toward stall control of multistage compressors, Day et al. [5] performed a careful study of stall inception in four high-speed multistage compressors and found that each compressor displayed different routes to stall. In addition to the long- and short-wavelength disturbances first identified by Day [6], they found high-frequency disturbances (10 to 13 times rotor frequency), shaft order perturbations, and near-instantaneous (in less than one rotor revolution) flow field breakdown as additional paths to stall. These complexities

made the prospects of active control or corrective control prior to stall seem rather poor for multistage compressors.

Despite these findings, two research teams have attempted compressor stall control on aeroengine compressors. Freeman, et al. [7] reported on stall control efforts for a VIPER engine using both steady and controlled recirculation. The VIPER engine is a single-spool turbojet with an 8-stage compressor of 5.25 pressure ratio. Air was recirculated from the fourth stage to the inlet, from the exit to the inlet, and from the exit to the fourth stage stator. When recirculating from middle to front, 8% of inlet massflow was used. When recirculating from exit to inlet, 5% of inlet massflow was used. The results indicated that controlled recirculation was more effective than steady bleed at controlling stall. Leinhos, et al. [8] performed stall control studies on the low-pressure compressor of a twin-spool turbofan engine using injected air from an external source as well as bleed from the high-pressure compressor. The low-pressure compressor consisted of two stages with a pressure ratio of 2.28. A doubling of the surge margin was demonstrated when injecting 5% of the design point massflow from an external source.

The focus of the present investigation is to demonstrate stall control using minimum amounts of recirculated air on a technology development multistage compressor operating at loading levels beyond those used in commercial aircraft engines (and well beyond the loading levels of the compressors used by Freeman and Leinhos). The first phase of the work involves the design of compact injectors that are flush with the endwall and fit within the axial gap between the stators and rotors of a multistage compressor. The second phase involves proof-of-concept evaluation of these injectors on a single stage transonic compressor using both an external air source and air recirculated from the exit of the stage. The final phase involves assessment of the recirculation concept on the multistage compressor operating between 78% and 100% of design speed. In this test air from an external source was steadily injected upstream of several rotor blade rows while compressor bleed was increased by an amount equivalent to the injected massflow. Feedback control of jet injection, using the high-speed actuators employed by Weigl [1] and Spakovszky [2,3], was also used to study the compressor dynamics and to reduce the amount of injected flow required for stability augmentation. Recirculation of hot bleed air was not attempted because the high-speed actuators were only capable of operating with ambient-temperature injected air.

SINGLE STAGE COMPRESSOR TESTS

Research Compressor

A transonic compressor stage was used for development testing of endwall flow recirculation. The stage tested, designated NASA stage 35, has 36 rotor blades, 46 stator blades, a rotor inlet tip radius of 25.4 cm, a hub-tip radius ratio of 0.70, a rotor aspect ratio of 1.19, and a rotor tip solidity of 1.3. The compressor was designed for axial inlet flow, and the inlet relative Mach number is 1.48 at the tip at design speed. The rotor tip clearance at design speed is 0.5 mm, which is 0.86% of tip chord. The compressor aerodynamic design and blade coordinates were reported by Reid and Moore [9].

Overall compressor performance measurements are reported in terms of total-to-static pressure ratio based on casing static pressures measured at 12 points around the annulus downstream of the stator. Inlet massflow is measured with a calibrated orifice plate located far upstream of the compressor inlet plenum. Both the inlet massflow to the compressor and the injector massflow are corrected to standard day conditions. The sum of these corrected massflows is the total massflow rate at the rotor face. Measurement uncertainties calculated from an analysis of measurement errors are: massflow 0.11 kg/sec and pressure 10^3 N/m². No attempt was made to measure compressor efficiency with injection because the flow exiting the stage is circumferentially non-uniform and exit flow conditions were measured with only two pressure and two temperature rakes.

The injector exit velocity is calculated using total pressure and temperature measured within the injector and a static pressure measured on the compressor casing just upstream of the rotor leading edge. Injector massflow is calculated by assuming a uniform velocity across the injector exit area (slug flow). A survey of the injector exit flow distribution performed with the injector coupled to a compressed air source verified that the discharge coefficient for the injector is near unity.

Compressor stability is typically assessed using stall margin, defined as either: 1) the change in massflow and pressure rise between the operating line and the stall line at a fixed rotational speed; or 2) the change in pressure rise between the operating line and the stall line at a fixed mass flow. However, an isolated stage in a compressor rig test does not have an operating line. We therefore choose to quantify changes in stability as the normalized change in stalling flow coefficient,

$$\Delta\phi_{\text{stall}} = ((\phi_{\text{stall}})_{\text{b}} - (\phi_{\text{stall}})) / (\phi_{\text{stall}})_{\text{b}},$$

where $(\phi_{\text{stall}})_{\text{b}}$ is the stalling flow coefficient for the baseline (no-injection) case. Note that this parameter is identical to the percentage change in the corrected stalling flow rate at the rotor face since

$$\phi = V_x / U_t = m / (\rho A_a U_t),$$

where A_a is the annulus area, m is the sum of the annulus and injector massflow rates (corrected to standard-day conditions), ρ is the density at standard-day conditions and U_t is the corrected tip speed.

Injector Development

The injectors used by Suder et al. [4] and Leinhos et al. [8] were located approximately two rotor chords upstream of the rotor leading edge and protruded into the flow path. Such injectors are not suitable for use in multistage compressors, where the spacing between blade rows is typically a fraction of a rotor chord. Therefore the first phase of the present effort focused on the design of compact injectors capable of generating a wall jet along the compressor casing.

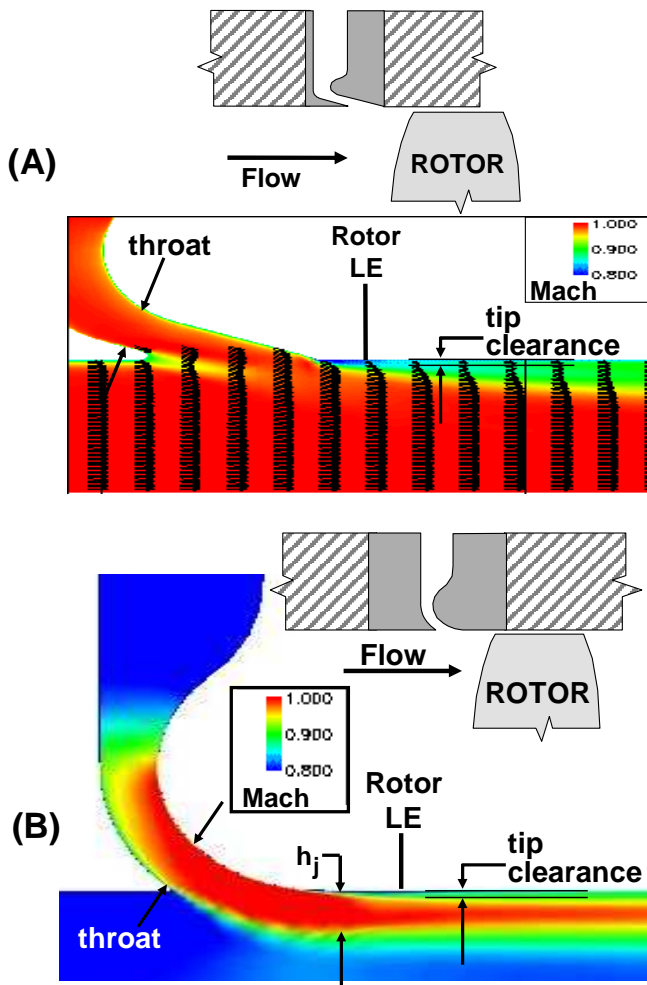


Figure 1 (A) CFD predictions of the wall jet flow from an angled slot injector flowing into a two-dimensional duct. (B) CFD predictions of the wall jet flow from a coanda injector flowing into a two-dimensional duct.

The first injector style evaluated featured an angled slot, set at a shallow pitch angle relative to the casing, as shown in Figure 1a. The injector throat is located at the injector exit, as shown in the figure. Also shown is a 3D Navier-Stokes prediction of the absolute Mach number on an axial-radial plane located at the injector centerline. The injector is choked in this simulation and is discharging into a two-dimensional duct that is also flowing at a Mach number of one. To correctly predict the penetration of the injector flow into the duct flow, the duct width was set to be much wider in the circumferential direction than the width of the injector. The injector throat height is equivalent to six times the height of a typical rotor tip clearance gap. This choice of throat height is arbitrary, but was chosen based on the earlier experience of Suder et al. [4]. The axial location that would be occupied by the rotor leading edge plane if this injector were installed in a multistage compressor is also shown. The predicted flow field indicates the presence of a small separation just upstream of where the rotor leading edge would be, followed by a larger region of relatively low momentum flow with a radial extent of 3-5 times the rotor tip

clearance. Since the design goal for the injector is to increase the axial momentum near the rotor tip, we concluded that a slot-type injector was not a viable design.

The second injector design we evaluated featured a downstream injector half with a circular arc that is tangent to the flowpath, as shown in Figure 1b. This injector design is based on the coanda effect, wherein the static pressure gradient across the curved streamlines within the injector works to keep the flow attached to the flowpath wall downstream of the injector. The predicted Mach number along the injector centerline plane is also shown in Figure 1b. This simulation result is for a choked injector flowing into a two-dimensional duct with a freestream Mach number of 0.5, which is similar to the axial Mach number found in the inlet stages of modern multistage compressors. The injector throat height is once again equivalent to six rotor tip clearance gap heights. The axial location that would be occupied by the rotor if this injector were installed in a multistage compressor casing is also shown, along with a typical tip clearance. The predicted flow field features a wall jet with high axial velocity in the region that would be occupied by the rotor blade tip. Note that the wall jet thickness is approximately equal to the injector throat height and that little or no mixing takes place in the streamwise region that would be occupied by the rotor. Based on this result, a set of coanda injectors was fabricated for evaluation in the NASA-Glenn single-stage axial compressor facility.

In order to capitalize on hardware used by Suder et al. [4], we considered only injectors that had the same width in the circumferential direction as those used by Suder. Each injector covered 3.5% of the circumference. The injectors also featured throat heights comparable to those used by Suder and had an injector aspect ratio, w/h , on the order of 18, where h is the injector throat height and w is the injector width. This high aspect ratio ensures that the flow leaving the injector is two-dimensional across much of the injector opening. CFD simulations of the type shown in Figure 1 also indicate that interaction between the annulus flow and the injected flow at the edges of the injector generates streamwise vorticity that tends to lift the injected flow away from the wall, which is an undesired result. The impact of this effect on injector performance is reduced when the aspect ratio of the injector is large.

Since recirculated air is expensive from a thermodynamic cycle point of view, it is desirable to achieve stability augmentation with a minimum amount of recirculated air. To this end, an optimization study of the injector throat width and the number of injectors was performed to determine the impact of these parameters on compressor stability. The injectors were supplied with air at ambient temperature from an external source for these tests. The results of the optimization study, performed at rotor design speed, are shown in Figure 2.

Figure 2a presents stability augmentation as a function of injected massflow. The abscissa is the total injected flow normalized by the annulus flow at the baseline (no-injection) stall point, while the ordinate is the normalized stalling flow coefficient described above. The data shown in black are for full-height injectors, with a throat width equal to 4% of the

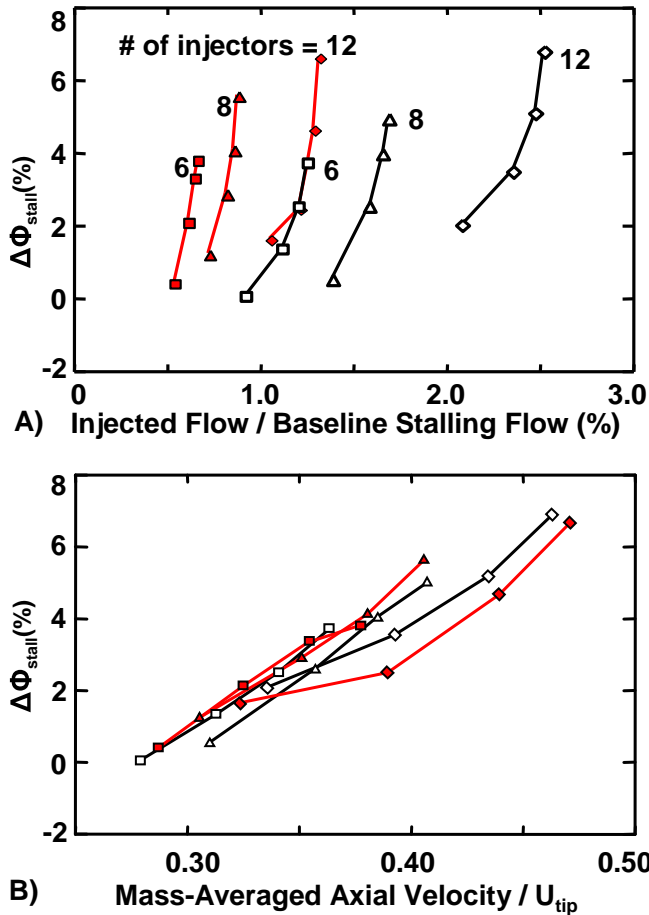


Figure 2 Change in stalling flow coefficient at design speed due to tip injection. Black symbols, full height injectors; red symbols, half-height injectors. (A) Stalling flow coefficient change as a function of injected massflow. (B) Stalling flow coefficient change as a function of circumferentially mass-averaged axial velocity at the rotor tip.

rotor blade span (6 times the rotor tip clearance). The data shown in red were obtained with an injector throat height equal to half of the full-height value. The maximum injected flow shown for each configuration is the flow for which the injectors are first choked, i.e. the absolute Mach number is unity at the injector throat. The injector exit static pressure matches the static pressure in the compressor flowpath for injector total pressures below the choking pressure. When the injector total pressure is raised beyond this level, the static pressure within the injector rises above that in the compressor flowpath, which will cause the injected jet to expand once it leaves the injector. To avoid this condition we arbitrarily set the initial injector choke point as the upper limit for injector operation. The results shown in Figure 2a indicate that:

- 1) Maximum stability enhancement increases almost linearly with the amount of the circumference covered by the injectors. Six injectors provide 21% circumferential coverage in the present case.

- 2) Stability enhancement does not scale with injected massflow or momentum. The half-height injectors yield the same increase in stability as the full-height injectors, even though they generate only half as much massflow and momentum.

The key to stability enhancement is shown in Figure 2b. The abscissa of this plot is the circumferentially mass-averaged axial velocity at the rotor leading edge, normalized by the rotor tip speed. From Suder et al. [4], the mass-averaged axial velocity is defined as

$$\overline{V_z} = \frac{[\rho_i(N * W * V_i^2) + \rho_c(\pi D - N * W) * V_c^2]}{[\rho_i(N * W * V_i) + \rho_c(\pi D - N * W) * V_c]}$$

where N is the number of injectors, W is the injector circumferential width, and D is the annulus diameter. V_i and ρ_i are the injected flow velocity and density respectively at the injector exit, and V_c and ρ_c are the annulus flow velocity and density evaluated at a distance $h/2$ (see Figure 1) from the casing. Figure 2b indicates that, over the range of injector geometric parameters investigated here, the compressor stability increase correlates fairly well with the increase in mass-averaged axial velocity that results from the injection. The mass-averaged axial velocity can therefore be used to make design decisions on injector count, injector circumferential width, and injector throat height as a function of injected massflow.

Recirculation Tests

In an installed compressor application, tip injectors would be supplied by recirculating air that was bled from the flowpath downstream of the compressor. A “stage recirculation” system was therefore designed for the NASA compressor facility to assess this concept. The system features a bleed slot located downstream of the stator, connected by a “bridge” to a coanda-style injector located just upstream of the rotor, as shown in Figure 3. The upper half of Figure 3 shows a meridional view of the bridge flow path, while the lower half shows a view looking radially inward at the plane of the rotor and stator blade tips. The bleed slot throat is four times wider than the injector throat and the bridge channel height, h_b , is five times that of the injector throat. These features, coupled with the large-radius turns in the bridge channel, serve to reduce the flow velocity and total pressure loss within the recirculation system.

Based on the results shown in Figure 2, six recirculating bridges were installed on the compressor. Half-height injectors were chosen in order to minimize the amount of recirculated air required to achieve a given degree of stability enhancement. Due to interference with existing hardware on the compressor case, the bridges were not uniformly spaced in the circumferential direction, as shown in Figure 4. This limitation is considered acceptable for purposes of this demonstration since a recirculation system installed on a production compressor would most likely also have non-uniform spacing between injectors due to interferences with existing peripherals. Non-uniform spacing also serves to reduce any aeromechanical excitation of the rotors by the injected jets. Both Suder [4] and

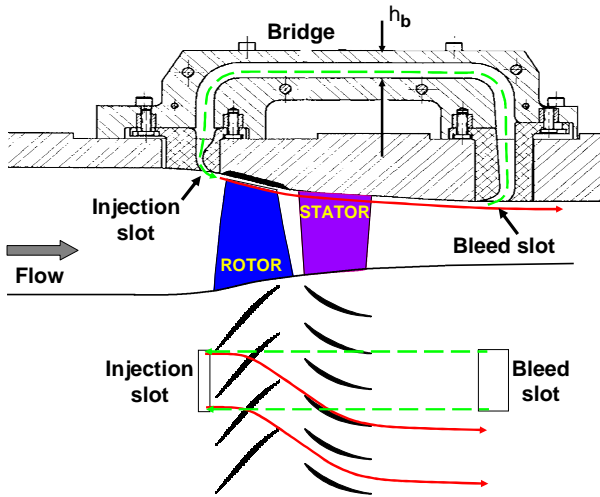


Figure 3 Scale drawing of the recirculated flow path through the single stage compressor. Green indicates the path of bleed air through the bridge; red indicates the path of injected air through the stage.

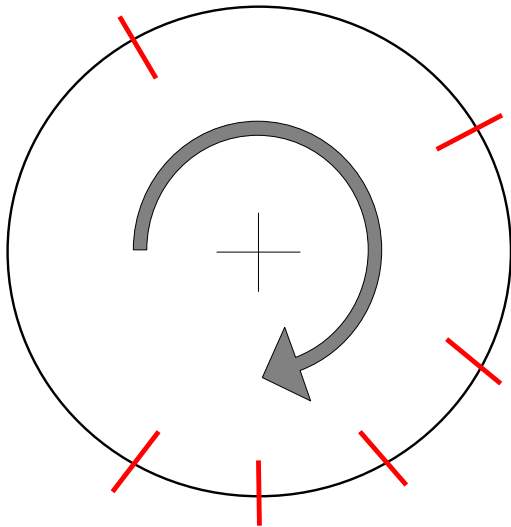


Figure 4 Circumferential distribution of recirculating bridges on the compressor case, showing direction of rotor rotation.

Freeman et al. [7] have shown that tip injection is still effective when the injectors have a non-uniform circumferential spacing. Suder in fact showed that, for a fixed number of injectors, stability enhancement is independent of the circumferential spacing between injectors.

Compressor performance with the bridges installed is compared to the baseline performance at 70% and 100% of design speed in Figure 5 for a clean, undistorted inlet flow. The stall line measured at speeds between 60% and 100% of design speed with and without recirculation is also shown. The abscissa is the total flow at the rotor face corrected to standard day conditions, which is the sum of the inlet flow measured far upstream and the recirculated flow. The baseline compressor

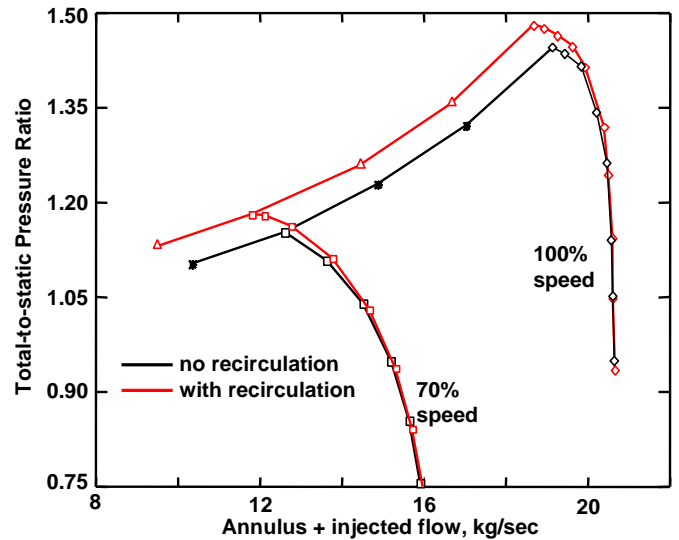


Figure 5 Single stage compressor pressure rise characteristics with recirculation. Black – compressor performance with no recirculation, Red – compressor performance with recirculation.

performance was determined with the injectors installed but capped off at the outer surface of the casing. Earlier measurements acquired with and without injectors installed indicated that there was no measurable difference in compressor performance or stalling flow due to the presence of the injectors when the injectors were not flowing.

Comparison of total pressure measurements made within the bridge return channel and near the casing downstream of the stator indicates that the bleed slot recovers about 30% of the dynamic head in the annulus flow exiting the stage. Calculated injector flow rates show that the flow through the injectors increases as the rotor pressure rise increases, with the maximum injected flow occurring at the stall point. The total flow through the injectors at 70% and 100% speed at the lowest pressure rise points shown in Figure 5 is 0.3% and 0.6% of annulus flow respectively. At the stall point the total injected flow is 0.9% of the annulus flow at both operating speeds. With the recirculation activated, the change in stalling flow coefficient is $\Delta\phi_{\text{stall}} = 6\%$ at 70% of design speed, while $\Delta\phi_{\text{stall}} = 2\%$ at design speed.

Since we are restricted to the use of ambient temperature air in the multistage compressor application described below, it is instructive to investigate the difference in injector performance when supplied by ambient-temperature air instead of warm recirculated air. To this end, the bridges were removed from the casing and a small plenum chamber was placed over each injector and fed from an external source with air at the compressor inlet temperature. The results are presented in Figure 6 for design speed. At the stall point this single stage generates just enough pressure rise to choke the injectors and the recirculation system is operating at a temperature ratio of $T_{\text{bleed}}/T_{\text{inlet}} = 1.31$. Since the choke

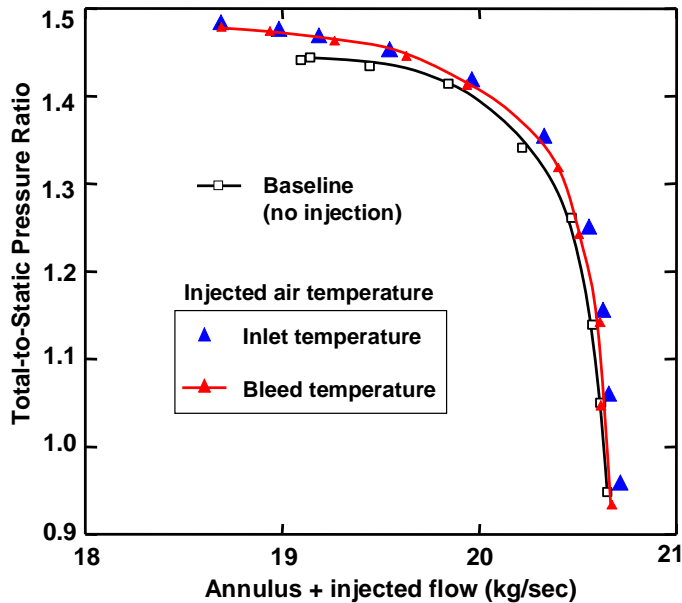


Figure 6 Comparison of injector performance at design speed when fed with inlet-temperature air and with recirculated air at bleed temperature.

condition is the upper limit we set for injector operating pressure, the results of Figure 6 verify that there is no temperature effect on injector performance over this range of injector operating pressures.

Due to the low pressure rise across the single stage at 70% speed, the injector Mach number generated using recirculated air is only 0.63, which yields a 6% reduction in the stalling flow coefficient of the compressor. As shown in Figure 7, the results obtained with external air injection at higher pressures indicate that a much greater increase in stable operating range can be achieved with these injectors when they are run at higher supply pressures. A 17% reduction in stalling flow coefficient could be expected when the injectors are choked. Therefore, in a multistage application a significant increase in part-speed stability could be achieved by feeding the injectors from a bleed located several stages downstream of the injector.

MULTISTAGE COMPRESSOR TESTS

Research Compressor

The multistage high-pressure compressor used to assess the performance of endwall recirculation was a six-stage aeroengine technology development compressor designed to replace a nine-stage production unit. The blading designs employed the latest three-dimensional aerodynamics, including forward-swept rotors and bowed, swept stators.

The compressor was tested in a compressor rig that included several features designed to model an aeroengine environment. Flow entered the compressor through an atmospheric inlet, and then passed through a settling chamber and a 10-strut inlet section that modeled the gooseneck between the low-pressure and high-pressure spools in the production

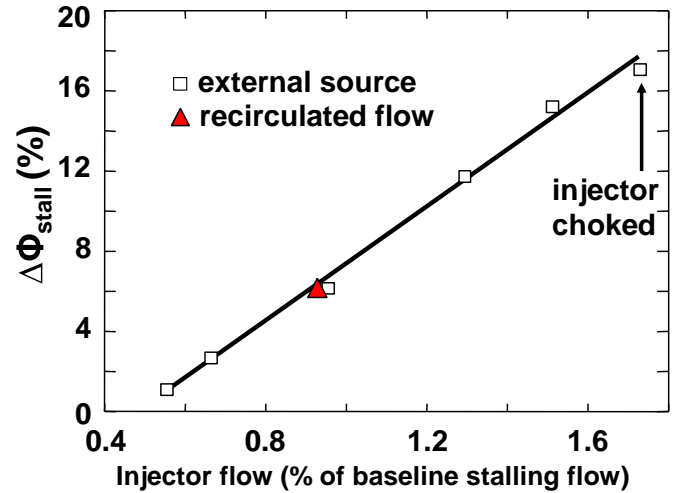


Figure 7 Stability increase as a function of injector flow at 70% speed. Injector Mach number for recirculated flow is 0.63.

engine. The inlet section also included a radial distortion screen that generated the pressure-only equivalent of the pressure and temperature profiles expected from the low-pressure compressor in the production engine. The rig hardware included a diffuser downstream of the last stage. A volume that models the combustion chamber volume in the production engine was located between the diffuser and the rig throttle valve to insure that the surge dynamics of the rig-test compressor were similar to those that would be encountered in the production engine. Customer bleed and low-pressure turbine cooling bleed were taken off behind the third stage. A high-pressure turbine cooling bleed was taken off behind the last rotor.

Massflow was measured by venturi flow meters located in the inlet housing upstream of the settling chamber. Inlet pressure and temperature were measured within the inlet strut section and corrected for strut loss to yield corrected flow conditions at the face of the inlet guide vane. Exit conditions were measured by total pressure and temperature rakes located downstream of the diffuser. Capacitance probes located over each rotor were used to monitor rotor tip clearance. Casing thermal growth was monitored during all injection tests and the thermal management capabilities of the test rig were used to maintain a constant tip clearance. Nominal clearance-to-chord ratio over rotor 1, 3, and 5 was maintained at 0.45%, 0.81%, and 1.93% respectively at design speed.

The objective of the tests described below was to assess to what extent recirculation could augment the compressor stability. Therefore, casing treatment that had been present over rotors 4, 5, and 6 was removed prior to the start of recirculation tests and replaced by solid inserts to reduce the high-speed stall margin of the machine.

Injection System

It is well-known that stage matching changes with spool speed in a multistage compressor, with front stages being

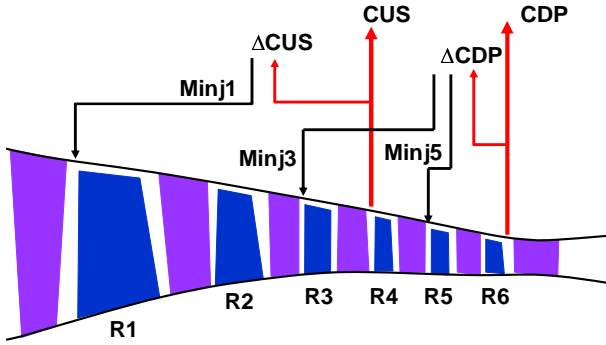


Figure 8 Schematic representation of simulated recirculation in the multistage compressor. Customer bleed, CUS, is incremented by an amount ΔCUS to account for massflow Minj1 injected into R1, and compressor discharge bleed, CDP, is incremented by an amount ΔCDP to account for massflows $\text{Minj3} + \text{Minj5}$ injected into Rotors 3 and 5.

loaded at part-speed conditions and rear stages being loaded at high-speed conditions. In order to provide stability enhancement over a wide speed range, coanda-style injectors were installed upstream of rotors 1, 3, and 5. Eight injectors covering 22% of the circumference were located upstream of rotor one, twelve injectors covering 23% of the circumference were located upstream of rotor 3, and twelve injectors covering 5% of the circumference were located upstream of rotor 5. Injectors upstream of rotors 1 and 3 were uniformly spaced around the circumference. Because of interference with other hardware on the casing, the rotor 5 injectors were not uniformly spaced, but rather were located in two groups of six with each group covering approximately 90° circumferentially. Because of the small interstage spacing in the rear of the machine, the rotor 5 injectors were actually located between stator 4 airfoils. All injectors on rotors 1 and 3 were controlled by the same high-speed valves and controller system used in the active control experiments of Weigl [1] and Spakovszky [2,3]. These injectors could therefore be operated in both a steady- and unsteady-injection mode as described by Weigl and Spakovszky. In unsteady mode, the injectors were used to explore the compressor dynamics and to attempt feedback-controlled injection. Rotor 5 injectors were operated in steady-injection mode only.

Because the high-speed valves in the injection systems for rotors 1 and 3 were not rated for operation with hot bleed air, ambient-temperature air from an external source was used for all injection. A separate air injection supply circuit was fabricated for each set of injectors (rotors one, three, and five). The total flow injected into a given rotor was measured by a venturi and was also calculated using pressure taps and thermocouples located in the injector bodies. Recirculation within the compressor was simulated in the rig as shown schematically in Figure 8. Customer bleed was increased by an amount that matched the injected airflow into rotor 1. Similarly, compressor discharge bleed flow was increased by an amount that matched the flow injected into rotors 3 and 5. The physical bleed flow amounts were scaled to the physical

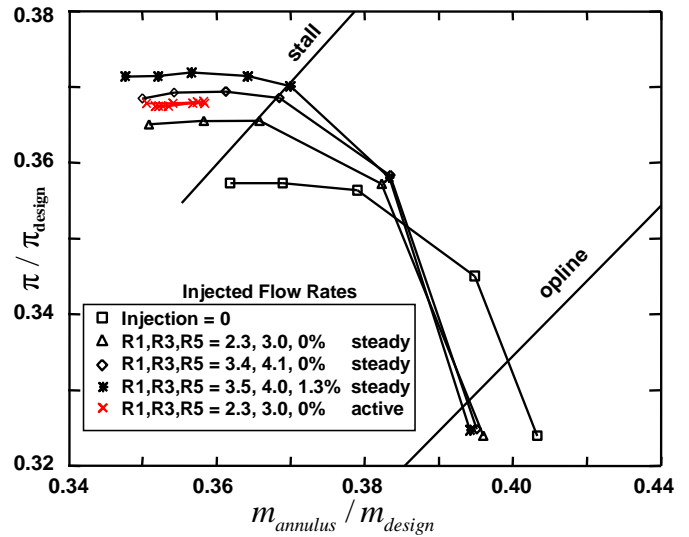


Figure 9 Pressure vs. flow characteristics at 78% speed with injection.

injected flow amounts by the factor $\sqrt{T_{bleed} / T_{inject}}$, which matches the bleed and injection massflows on a corrected flow basis. The results shown in Figures 6 and 7 indicate that although we are using ambient-temperature air to supply the injectors, we can expect the same impact on compressor stability as would be achieved using heated air from true recirculation.

The injection/bleed approach described above divides the compressor into two “blocks”. The front block consists of stages 1-3 with injection on rotors 1 and 3 and customer bleed taken just behind the front block. The rear block consists of stages 4-6 with injection on rotor 5 and bleed taken behind rotor 6. As will be discussed below, the true benefit of the recirculation modeled during the rig tests turned out to be the ability to throttle the front and rear blocks independently and thereby improve the stage matching at any given speed.

Steady Injection Results

The results of tip injection tests at 78% of design speed are shown in Figure 9. The abscissa is the annulus flow measured in the inlet strut section upstream of the compressor normalized by the flow at the design speed operating point, $m_{annulus} / m_{design}$, while the ordinate is the total pressure ratio normalized by the pressure ratio at the design speed operating point, π / π_{design} . The operating line derived during the compressor design and the stall line determined from an earlier test of the compressor with no injectors installed is also shown.

In the single stage compressor tests described above, it was relatively straightforward to calculate a total corrected inlet flow at the rotor face that accounted for the sum of the rig annulus flow and the injected flow. In the multistage machine, due to the complexity of massflow addition through injectors at a different pressure upstream of each injected rotor blade row and massflow extraction through bleeds at different pressures

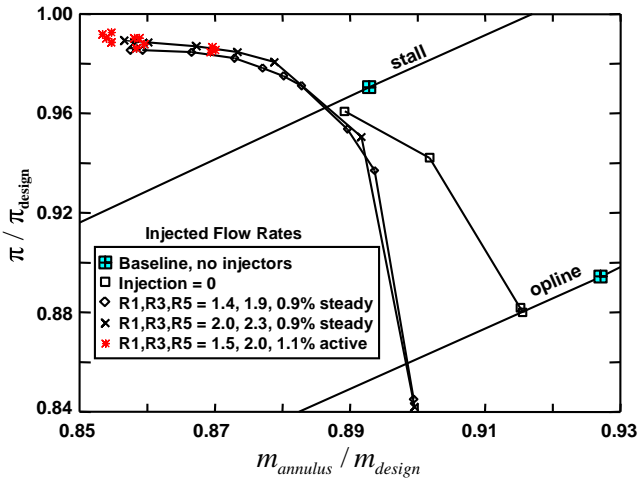


Figure 10 Pressure vs. flow characteristics at 97% speed with and without injection.

and temperatures, no attempt is made to calculate a total corrected inlet flow to the compressor. Figure 5 shows that the total flow (rig inlet flow + injected flow) at the rotor face does not change when injection is added to the compressor. The inlet flow therefore drops as injection is added. The pressure vs. flow characteristics shown in Figure 9 therefore show a shift to lower flow with injection present because the massflow being plotted is the inlet flow into the rig.

Three different steady injection cases and one active control case are shown in Figure 9. In the active control case (data points shown in red), unsteady injection was implemented by using a control computer to command the position of the high-speed valves that meter the flow to the rotor 1 and rotor 3 injectors.

The injected flow rates shown in the table within the figure are normalized by the inlet flow measured at the operating line when no injection was present. The stall margin for each injection configuration is summarized in the Appendix. The first two injection cases involve different amounts of injection into rotors 1 and 3, with the injectors being choked in the second case. The third case involves injection into rotor 5 as well, with rotor 5 injectors choked. Note that although one would expect the front block of the compressor to be loaded relative to the rear block at this speed, injection into rotor 5 has some impact on the stall point. This is one manifestation of the fact that the injection is improving stage matching within the compressor.

Analysis of the active control results will be presented in the next section. However, it is worth noting here that unsteady injection is more effective than steady injection in that, for the same amount of injected flow, greater pressure rise is achieved with unsteady injection than with steady injection.

Injection results measured at 97% speed are shown in Figure 10. Baseline data points on the operating line and stall line taken before installation of the injectors are shown in the figure as well as similar data points taken with the injectors installed but not flowing. Comparison of these points indicates

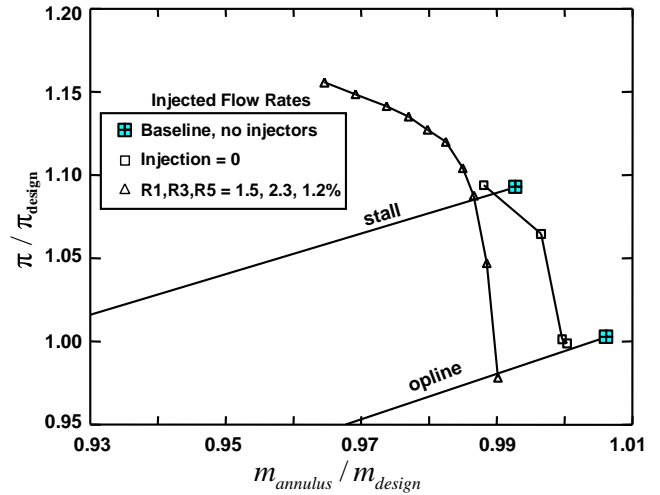


Figure 11 Pressure vs. flow characteristics at 100% speed with and without injection.

a flow shift along the operating line of approximately 1% after injector installation. Since the compressor underwent a significant amount of running between measurement of the baseline performance and the performance with injectors, some of this shift may be due to deterioration of clearances within the machine. However, this shift might also be due to pumping of the injector cavities by the passing of the rotors located just downstream of each injector. Three injection cases are also shown in the figure. In the first case, the injector absolute Mach numbers for rotors 1, 3, and 5 were approximately 1.0, 0.6, and 0.8 respectively. In the second case the rotor 1 injector total pressure was increased to 50% above the total pressure required to choke the injector in order to drive more injector flow into rotor 1 and thereby unload the front block of the compressor. During these tests, it became apparent that high injector Mach number did not always provide the best improvement in stability. The true benefit of the injection/bleed approach was once again found to be the ability to independently control the throttling of the front and rear blocks.

Injection results acquired at design speed are shown in Figure 11. The injector flow rates chosen were those that gave the best results at 97% speed. Injector Mach numbers into rotors 1, 3, and 5 for the injection case shown was 1.2, 0.8, and 1.0 respectively.

Based on the success of the injection system at increasing compressor stability in the high-speed portion of the operating envelope, the ability of the system to recover stability lost due to increased rotor tip clearance was assessed. Using the thermal management capability of the test facility, the clearance/chord ratio over rotors 1, 3, and 5 at 97% speed was increased as shown below:

Rotor	1	3	5
Nominal clearance/chord	0.49%	0.77%	2.04%
Increased clearance/chord	0.58%	1.78%	3.61%

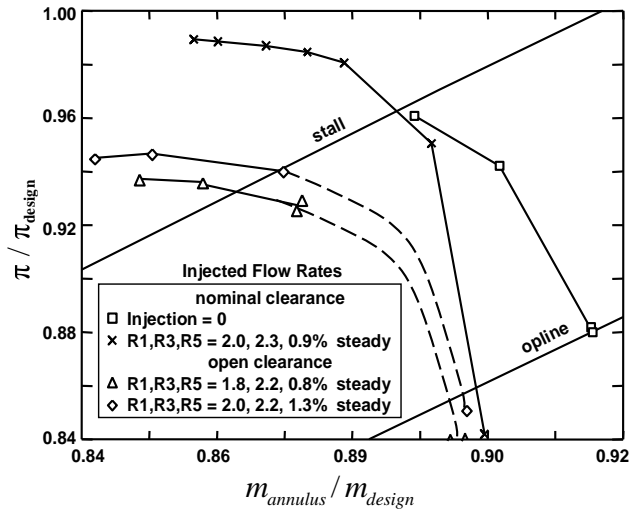


Figure 12 Pressure vs. flow characteristics at 97% speed with injection for increased rotor tip clearance.

The impact of tip injection on the pressure-flow characteristics of the nominal and increased clearance cases are shown in Figure 12. The increased clearance resulted in a loss in pressure rise as would be expected. However, tip injection not only recovered the surge margin typically lost by increased tip clearance, but also extended the stable operating range beyond that of the baseline compressor. These results indicate that an endwall recirculation system is capable of restoring the stable operating range lost due to open rotor tip clearances that arise as compressors deteriorate.

Active Control Results

Stall and surge dynamics were monitored using high-response pressure transducers. Eight transducers were located around the circumference upstream of rotors 1, 2, and 3 while four transducers were located upstream of rotors 4, 5, and 6. These transducers were also used as inputs to the stage 1 and stage 3 injector control systems during closed loop active control.

Two separate systems were used for data acquisition and control. A high-speed A/D system capable of 32 channel acquisition was used at a sample rate of 10 KHz and filtered at 4 KHz with a 16 bit resolution. A separate PC-based control computer (originally described by Wiegl [1]) also was used to digitize and resolve the data at a 2.5 KHz sampling rate for closed loop control application.

Compressor dynamics were investigated at 78% and 97% of design speed by acquiring pressure transducer signals while continuously throttling the compressor into stall with and without injection present. The purpose of this was two-fold: first, to visually identify the stalling stage of the compressor; second to identify the stall dynamics of that stage and if they changed during injection. Since controlled injection was installed at stages 1 and 3, we concentrated on the information from these two stages only. The study at 78% speed revealed several behaviors from the casing static pressures upstream of rotor 1 and rotor 3.

Figure 13 shows casing static pressure data acquired near stall. The abscissa is time measured in rotor revolutions before stall and the ordinate is pressure in arbitrary units. The top two traces are from transducers located ahead of rotor 1 while the bottom two traces are from transducers located ahead of rotor 3. At 78% speed with no injection, a short-wavelength disturbances or “spike” grows into stall at rotor 1. Similarly, rotor 3 shows a spike disturbance. Upon close inspection of the pressure traces, rotor 3 stalls 20 milliseconds (approximately 4 rotor revolutions) ahead of rotor 1 when no injection is present.

The compressor dynamics were next examined at 78% speed with steady injection at rotors 1, 3, and 5. In Figure 14, the pressure measurements show that modal disturbances are present ahead of rotor 3 but no disturbances are present ahead

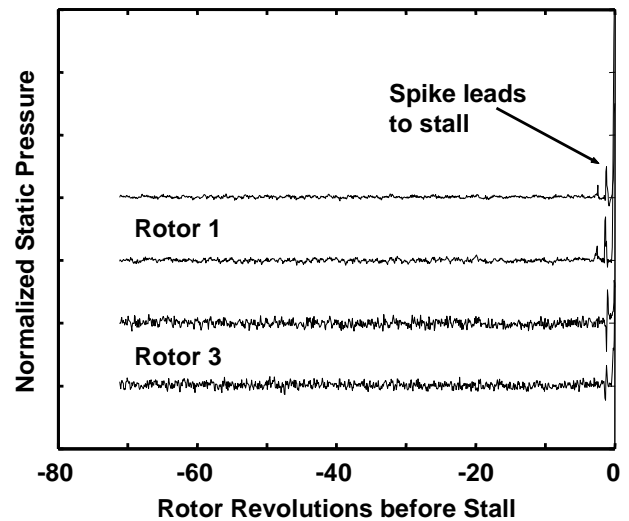


Figure 13 Static pressure disturbances upstream of rotors 1 and 3 at 78% speed with no injection.

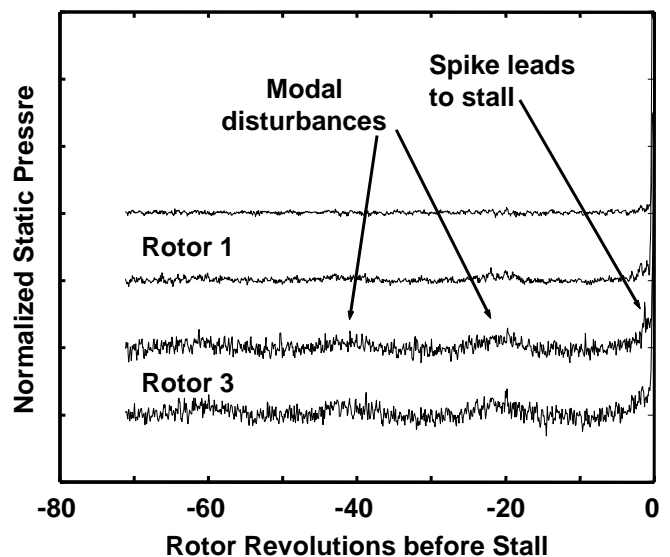


Figure 14 Static pressure disturbances upstream of rotors 1 and 3 at 78% speed with steady injection into rotors 1, 3, and 5.

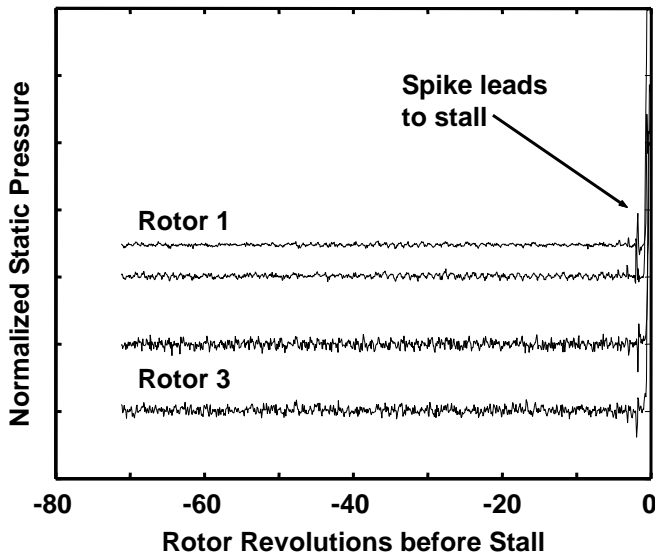


Figure 15 Static pressure disturbances upstream of rotors 1 and 3 at 78% speed with feedback-controlled injection into rotor 3.

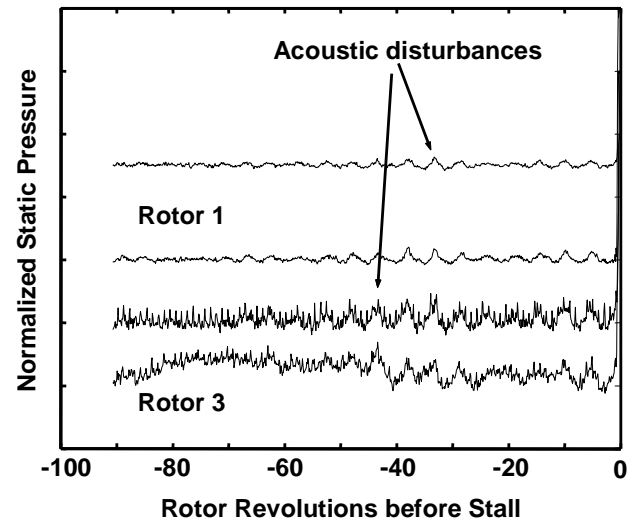


Figure 17 Static pressure disturbances upstream of rotors 1 and 3 at 97% speed with steady injection into rotors 1, 3, and 5.

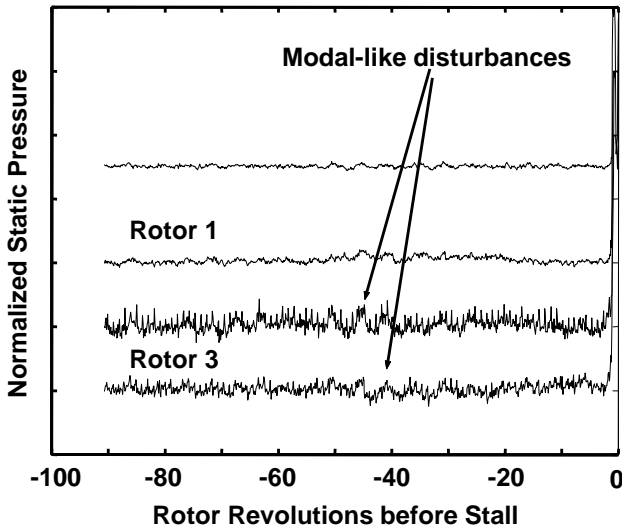


Figure 16 Static pressure disturbances upstream of rotors 1 and 3 at 97% speed with no injection.

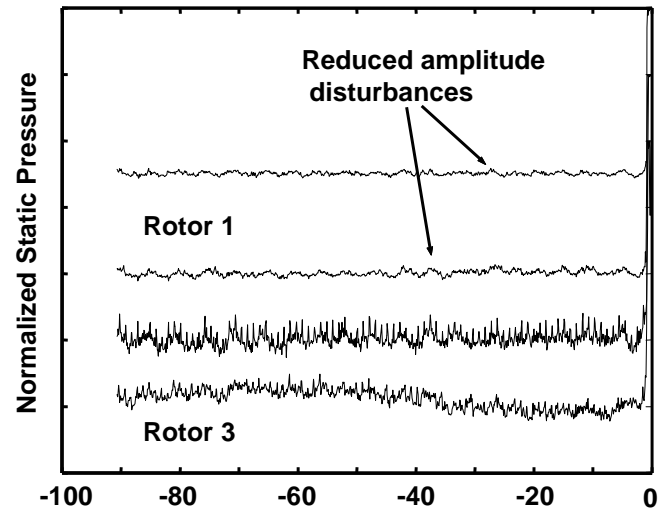


Figure 18 Static pressure disturbances upstream of rotors 1 and 3 at 97% speed with steady injection into rotor 3.

of rotor 1. Again, rotor 3 stalls 20 milliseconds before rotor 1. The compressor characteristic for this data appears in Figure 9.

From this information we see that rotor 3 appears to control the stall at part speed condition, whether or not injection is applied. Further, steady injection makes the stage 3 dynamics more modal and more conducive to a linear control scheme. Therefore, for this condition, we had an opportunity to apply a wave-launching, closed loop, constant gain control. This was applied only at rotor 3. The amplitude and phase was selected based on the amplitude of modal disturbances ahead of rotor 3 and from open-loop system identification of rotating stall frequencies. The closed loop scheme launches a sinusoidal disturbance to counteract the modal pre-stall behavior at rotor 3.

In Figure 15 we examine 78% speed data with controlled injection at rotor 3, (using this controller as first reported by Weigl [1]). The rotor 1 pressures now have spike disturbances that completely rotate around the circumference and lead to stall. Rotor 1 is now controlling the stall and rotor 1 stalls before rotor 3. The compressor characteristic for this case shows a pressure rise above the injection configuration using steady injection, but with a similar range extension. This would indicate that the compressor now stalls due to dynamics at rotor 1. This also shows that the dynamics of controlled injection provide a range extension equivalent to using steady injection, but with a reduction in the injected mass flow.

We also investigated pre-stall dynamics at a 97% speed condition. At this speed, pre-stall pressure signals show

unsteady “modal” disturbances ahead of rotor 3, as shown in Figure 16. Upon further investigation, these modal disturbances were not traveling and appear to be surge or acoustic waves at a 48 Hz frequency, which is close to the resonance frequency that would be expected for an acoustic disturbance with a wavelength equal to the length of the test rig settling chamber. When steady injection is applied to rotors 1, 3 and 5, strong acoustic disturbances appear ahead of rotors 1 and 3 as shown in Figure 17. Rotor 3 stalls ahead of rotor 1, even with steady injection present.

To identify the preferred stage for closed loop control, we examined a case of steady injection only at rotor 3. As shown in Figure 18, the acoustic disturbances that were prevalent when injection was applied to rotors 1, 3, and 5 are now lower in amplitude than those shown in Figure 17. It appears that injection at rotor 3 can manipulate behavior for improved active control results, since our control scheme is based on damping modal disturbances. Therefore, active control at rotor 1 was performed while using steady injection at rotor 3 and 5.

From the compressor characteristic in Figure 10, it is shown that simple, constant gain control, even at 97% speed, is effective in changing the rotor 1 and rotor 3 dynamics to improve stability. Active control oscillates about a mean open flow condition, and uses less mass flow than steady injection at full open condition. This result is significant. Active control reduced the customer bleed to feed the unsteady controlled injection but achieved the same stalling mass flow condition as steady injection.

DISCUSSION

The stage recirculation system developed for the single stage compressor is similar in function to recirculating rotor casing treatments described by Koff [10] and Akhlaghi et al. [11], but has several differences relative to such treatments. First, the driving pressure for the flow recirculated through a casing treatment must be generated by the rotor over which the casing treatment resides. Results from Suder et al. [4] and the present investigation indicate that tip injection is most effective when the injector is choked, which requires approximately a two-to-one pressure ratio between the injector supply pressure and the static pressure upstream of the rotor tip. This pressure ratio may not be available across a single rotor row in the rear stages of a multistage compressor, and may also not be available from any rotor at a part-speed operating condition. However, the bridge design shown in Figure 3 can be extended axially to connect an injector to a bleed located two or more stages downstream to insure a pressure difference between the bleed and injection locations that is capable of choking the injector under all compressor operating conditions. The second difference in the stage recirculation system stems from placing the bleed location downstream of the stator. Since the compressor flow has been turned back to axial by the stator, the recirculating bridge is a simple axial connection between the bleed and injection slots. In a recirculating casing treatment, the bleed flow is taken from the high-swirl region just downstream of the rotor, and de-swirl vanes are required in the return channel over the rotor tip to turn the flow back to axial before injecting into the rotor tip. The last difference in the stage recirculation system results from the finite circumferential

extent of the bleed and injection slots. As shown in the lower half of Figure 3, by properly choosing the circumferential width of these slots, the injected flow passes through the rotor only once, and is not re-ingested by the bleed slot. In contrast, a recirculating casing treatment that covers the entire circumference continuously re-ingests flow that has already been injected into the rotor, which can result in increased casing temperatures over the rotor tip. For recirculation across a single stage, the current approach will generate less temperature increase across the rotor tip than a recirculating casing treatment. This advantage will be reduced when recirculating across multiple stages. In that case, the temperature of the injected flow will be set by the pressure ratio across the bridge and the efficiency of the compressor stages located between the bleed and injection slots.

Based on the differences discussed above, Hathaway [12] has recently designed a recirculating casing treatment that combines the recirculating features of Koff's design [10] and the discrete circumferential bleed and injection of the stage recirculation system shown here.

CONCLUSIONS

Recirculation of endwall flow has been shown to provide extension of the stable operating range of high-speed, highly-loaded compressors. A single stage transonic compressor rig was used for development testing of compact injectors that do not protrude into the compressor flowpath. The rig was also used to evaluate the effects of injected air temperature on stability augmentation. The single-stage results clearly indicate that recirculation extends the stable operating range of the stage to lower corrected flows than can be achieved without recirculation.

A highly-loaded multistage compressor rig was then used to study the effects of recirculation in a multistage environment, using both steady and unsteady injection into multiple rotor rows within the compressor. Recirculation was modeled in this rig through a combination of injection from an external source and increased compressor bleed. Individual stage characteristics (not included herein) indicate that the stall margin improvements obtained in this work resulted more from an improvement in matching between stages than from a reduction in the stalling massflow of individual rotor blade rows. This leads us to conclude that a recirculation system must be carefully designed for a particular multistage compressor application. Such a design should consider the throttling characteristics of each stage when determining the stage from which to take bleed flow for recirculation and the stage in which to re-inject the recirculated flow.

The following conclusions can be drawn from this investigation:

- Compressor stability can be augmented when injecting flow over only a portion of the compressor circumference. The key to effective stability improvement is an increase in the circumferential mass-averaged axial velocity at the rotor tip.

- Injectors fed with air at the compressor inlet temperature have the same effectiveness as those fed from air that is bled from a downstream location in the compressor flowpath. Single stage testing verified this behavior across an injector pressure ratio range of $1.0 < PR_{\text{injector}} < 2.0$, and across an injector temperature ratio range of $1.0 < TR_{\text{injector}} < 1.30$.
- Recirculation within a highly-loaded multistage compressor provides an effective means of increasing stability across a range of operating speeds. Individual stage characteristics indicate that recirculation enables the ability to throttle individual stages relative to one another, thus improving stage matching.
- Unsteady injection increases stability more than steady injection and is capable of changing the unsteady near-stall dynamics of a multistage compressor.

ACKNOWLEDGMENTS

The authors would like to thank Mr. Peter Szuch, Mr. Andrew Breeze-Stringfellow, Mr. Dave Gorsham, Mr. Alan Barile, and Mr. Thomas Gallagher of General Electric Aircraft Engines for their support during installation and test of the multistage compressor. We also acknowledge the support of Mr. Tom Compton and Mr. Steve Taylor of General Electric for design and fabrication of compressor casing and test facility adaptations. The assistance of Mr. Rick Brokopp, Mr. Dave Williams, Mr. Helmi Abulaban, Mr. Randy Thomas, and Mr. John Jones during injector development at NASA Glenn Research Center is also acknowledged. The financial support of the Air Force Integrated High Performance Turbine Engine Technology program through Mr. John Lueke is also gratefully acknowledged.

REFERENCES

- [1] Weigl, H. J., Paduano, J. D., Frechette, L. G., Epstein, A. H., Greitzer, E. M., Bright, M.M., and Strazisar, A.J., 1998, "Active Stabilization of Rotating Stall and Surge in a Transonic Single Stage Axial Compressor," ASME Journal of Turbomachinery, Vol. 120, No. 4, pp. 625-636.
- [2] Spakovszky, Z.S., Weigl, H.J., Paduano, J.D., van Schalkwyk, C.M., Suder, K.L., and Bright, M.M., 1999, "Rotating Stall Control in a High-Speed Stage with Inlet Distortion: Part I – Radial Distortion," ASME Journal of Turbomachinery, Vol. 121, pp. 510-516.
- [3] Spakovszky, Z.S., van Schalkwyk, C.M., Weigl, H.J., Paduano, J.D., Suder, K.L., and Bright, M.M., 1999, "Rotating Stall Control in a High Speed Stage with Inlet Distortion: Part II – Circumferential Distortion," ASME Journal of Turbomachinery, Vol. 121, pp 517-524.
- [4] Suder, K.L., Hathaway, M.D., Thorp, S.A., Strazisar, A.J., and Bright, M.M., "Compressor Stability Enhancement Using Discrete Tip Injection," ASME Journal of Turbomachinery, Vol. 123, No. 1, pp. 14-23, January, 2001.
- [5] Day, I.J., Breuer, T., Escuret, J., Cherrett, M., and Wilson, A., 1999, "Stall Inception and the Prospects for Active Control in Four High Speed Compressors," ASME Journal of Turbomachinery, Vol. 121, pp 18-27.
- [6] Day, I.J., 1993, "Stall Inception in Axial Flow Compressors," ASME Journal of Turbomachinery, Vol. 115, pp. 1-9.
- [7] Freeman, C., Wilson, A.G., Ivor J. Day, I.J., and Swinbanks, M.A., 1998, "Experiments in Active Control of Stall on an Aeroengine Gas Turbine," ASME Journal of Turbomachinery, Vol. 120, No. 4, pp. 637-647.
- [8] Leinhos, D.C., Scheidler, S.G., Fottner, L., Grauer, F., Hermann, J., Mettenleiter, M., and Orthmann, A., 2002, "Experiments in Active Control of a Twin-Spool Turbofan Engine"
- [9] Reid, L. and Moore, R. D., 1978, "Performance of Single-Stage Axial-Flow Transonic Compressor With Rotor and Stator Aspect Ratios of 1.19 and 1.26, Respectively, and with Design Pressure Ratio of 1.82," NASA TP 1338.
- [10] Koff, S. G., Mazzawy, R. S., Nikkanen, J. P., Nolcheff, N. A., "Case Treatment for Compressor Blades. " U.S. Patent 5,282,718, Feb. 1, 1994.
- [11] Akhlaghi, M., Elder, R., and Ramsden, K., 2003, "Effects of a Vane-Recessed Tubular-Passage Passive Stall Control Technique on a Multistage, Axial-Flow Compressor: Results of Tests on the First Stage With the Rear Stages Removed," ASME Paper No. GT2003-38301, IGTI Turbo Expo, Atlanta, GA.
- [12] Hathaway, M.D., 2002, "Self-Recirculating Casing Treatment Concept for Enhanced Compressor Performance," ASME Paper No. GT-2002-30368, IGTI Turbo Expo, Amsterdam, The Netherlands.

APPENDIX

The following table summarizes the stability changes achieved with injection on the multistage compressor. Stall margin is defined as $SM = (m_{opline} / m_{stall})(\pi_{stall} / \pi_{opline}) - 1$, where m is massflow, π is total pressure ratio, and subscripts *opline* and *stall* refer to conditions at the operating line and stall line respectively for each injection configuration. For each compressor operating speed, the injection flow rate into each rotor is normalized by the inlet flow rate on the operating line for the baseline (no injection) case.

Configuration	Rotor 1	Rotor 3	Rotor 5	Stall margin
78% speed				
Baseline	0	0	0	18%
Steady injection	2.3%	3.0%	0	25%
Steady injection	3.4%	4.1%	0	26%
Steady injection	3.5%	4.9%	1.3%	28%
Active control, unsteady injection	2.3%	3.0%	0	26%
97% speed				
Baseline, no injectors installed	0	0	0	13%
Baseline, injectors installed	0	0	0	12%
Steady injection	1.4%	1.9%	0.9%	20%
Steady injection	2.0%	2.3%	0.9%	21%
Active control, unsteady injection	1.5%	2.0%	1.1%	21%
100% speed				
Baseline, no injectors installed	0	0	0	10%
Baseline, injectors installed	0	0	0	12%
Steady injection	1.5%	2.4%	1.2%	21%
97% speed open clearance				
Nominal clearance	2.0%	2.3%	0.9%	21%
Open clearance	1.8%	2.2%	0.8%	17%
Open clearance	2.0%	2.2%	1.3%	16%